FUNDAMENTAL STUDY ON THE RELATIONSHIP BETWEEN WOODEN STRUCTRES DAMAGE AND STRONG MOTION INDICES

Kazi R. KARIM[1], Masayuki KOHIYAMA[2] and Fumio YAMAZAKI[3]

ABSTRACT: This paper presents the relationship between the wooden structures damage and strong motion indices. The damage classes are defined by using thresholds of maximum inter-story displacement angles. Nonlinear time history analyses of nine hundred input motions are applied for twenty-five SDOF wooden structures, of which secant natural periods at deformation angle of 1/120rad range from 0.1s to 2.5s with 0.1s interval. The damage estimation accuracy of the seismic indices is evaluated quantitatively based on the slopes of the normalized regression logit models, which has the logistic distribution of binary regression models. It is found that the spectral accelerations considering the elongation of natural periods show higher correlation with the damages. Based on this observation, a new seismic parameter is proposed, which may be very useful for earthquake damage estimation of wooden structures.

Key Words: input ground motion, strong motion parameter, wooden structure, dynamic analysis, logit model

INTRODUCTION

To construct a relationship between earthquake ground motion and structural damage, a data set comprising inputs (strong motion parameters) and outputs (structural damage) is necessary. However, correlating the ground motion indices with the observed damage in a mathematical form is not easy because of large uncertainty involved and the relationship must be highly nonlinear. There are two approaches for doing this: 1) collect actual earthquake records and damage data to develop a regression model and 2) perform earthquake response analyses for given inputs and models and obtain the resultant damage (outputs). The former is more convincing because it uses actual damage data, and Tong and Yamazaki (1995), Yamazaki *et al.* (2000), etc. employed this. However, earthquake records obtained near structural damage are few, and the structures with various natural periods exhibit a large variety of damage states. With the latter, since it is not based on actual observations, much care should be taken in selecting structure models and input motions. For the all difficulties, it is easier to prepare well-distributed data set, and this approach is used in this study.

Selection of input motion parameters to correlate with the structural damage is important, but it is not an easy task. The peak ground acceleration (*PGA*) and peak ground velocity (*PGV*) are commonly used indices to describe the severity of the earthquake ground motion. However, it is well known that a large *PGA* is not always followed by severe structural damage, especially for long-period structures. Similarly, a large *PGV* is not always followed by severe structural damage, especially for the input

[1] Postdoctoral Fellow
[2] Research Associate
[3] Associate Professor

motion including permanent fault displacements (Loh *et al.*, 2000). Other indices of earthquake ground motion, e.g., equivalent velocity (V_E) related to seismic energy (Uang and Bertero, 1990), peak ground displacement (*PGD*), time duration of strong motion (T_d) (Trifunac and Brady, 1975), Spectrum Intensity (*SI*) (Housner, 1959; Katayama *et al.*, 1988), and central periods (Kamiyama, 1996; Nakamura *et al.*, 2002) can be considered in damage estimation (Molas and Yamazaki, 1995).

The focus of this study is to investigate the characteristics of ground motion parameters with respect to wooden structures damage. As mentioned earlier, since the relationship between ground motion indices and resulting damage is difficult to express in a mathematical form, a numerical procedure is applied for this problem. The story displacement angles from nonlinear time history analyses for nine hundred input motions of twenty-five SDOF wooden structures are used to represent the damage. The procedure using a logistic regression analysis is described to identify quantitatively the input parameters that have greater influence on the damage of wooden structures. Based on the results of the numerical analyses, the new ground motion index is proposed, which is specialized for the damage estimation of wooden structures.

INPUT GROUND MOTIONS

Earthquake records

For nonlinear dynamic response analyses and to have a well-distributed data set, 300 strong motion records with three scale factors, i.e., 1.0, 1.5, and 2.0, a total of 900, are used as the input motions. The records were selected from six earthquake events: the 1995 Hyogoken Nanbu (Kobe) of Japan, the 1994 Northridge of USA, the 1993 Kushiro-Oki of Japan, the 1987 Chibaken-Toho-Oki of Japan, the 1999 Chi-Chi of Taiwan, and the 2000 Tottoriken Seibu of Japan earthquakes. Note that the records were selected from all these earthquake events on the basis of a larger PGA. The summary of the earthquake records used in this study is shown in **Table 1**.

Table 1. Summary of the earthquake records used in this study

No.	Earthquake Event	Event Date	M_W[+]	No. of Records
1	Chibaken-Toho-Oki	17/12/1987	6.5	50
2	Kushiro-Oki	15/01/1993	7.6	50
3	Northridge	17/01/1994	6.7	50
4	Hyogoken Nanbu (Kobe)	17/01/1995	6.9	50
5	Chi-Chi	20/09/1999	7.7	50
6	Tottoriken Seibu	06/10/2000	6.6	50

[+]Moment magnitude

Ground motion indices

As the indices of ground motion severity, the Peak Ground Acceleration (A_{max}), Peak Ground Velocity (V_{max}), Spectrum Intensity (*SI*), Peak Product of Ground Acceleration and Velocity ($(AV)_{max}$), Japan Meteorological Agency (JMA) seismic intensity (I_{JMA}), Equivalent Velocity (V_E), Acceleration Response Spectrum (S_a), Velocity Response Spectrum (S_v), and Displacement Response Spectrum (S_d) of the input ground motions are considered. Note that the *SI* (Katayama *et al.*, 1988), I_{JMA} (JMA, 1996), and V_E (Uang and Bertero, 1990) are defined as follows:

SI: The Spectrum Intensity *SI* is calculated as the area under the relative-velocity response spectra of 20 percent damped Single-Degree-of-Freedom (SDOF) systems with natural periods between 0.1s to 2.5s. Katayama *et al.* (1988) redefined it by dividing by the period interval as follows in order to

emphasize its characteristics as an average velocity response of structures:

$$SI = \frac{1}{2.4}\int_{0.1}^{2.5} S_v(h=0.2,T)dT \tag{1}$$

I_{JMA}: The JMA seismic intensity scale (I_{JMA}) was revised recently (JMA, 1996). First, the Fourier transform is applied for the selected time window for the three-components of acceleration time histories. Then, a band-pass filter, which is the combination of a period-effect, high-cut, and low-cut filters, is applied in the frequency domain. After taking the inverse Fourier transform, the effect of the duration (τ) was considered for a vectorial composition of the three-components that is made in the time domain. Considering an acceleration value a_0 having total duration τ satisfying the condition $\tau(a_0) \geq 0.3\text{s}$, the JMA seismic intensity (I_{JMA}) is calculated by using **Equation (2)** as a real (continuous) number

$$I_{JMA} = 2.0\log a_0 + 0.94 \tag{2}$$

It should be noted that since only one component of each earthquake record is used in the time history analysis, hence, the three-components of each earthquake record in **Equation (2)** reduces to only one.

V_E: The equivalent velocity is calculated from the total input energy (E_I) of the earthquake ground motion along with the total mass m of the structure, and it is defined as

$$V_E = \sqrt{\frac{2E_I}{m}} \tag{3}$$

STURUCTURE AND DAMAGE MODELS

Structure models

A total of twenty-five wooden structures are used in this study. The models are selected with respect to the secant structural period that ranges from 0.1s to 2.5s with 0.1s interval, where the secant structural period ($T_{1/120}$) is defined at the story deformation angle (γ) equal to 1/120rad. A total of 20,000kg mass is assumed with a story height of 275cm for the all structure models. Each structure model consists of two springs, viz., slip spring (K_s) and polylinear spring (K_p). The force vs. story displacement angle relationship of wooden structures are well expressed by the combination spring of slip and polylinear springs and the model proposed by Suzuki and Nakaji (1997) is employed in this study, in which the resisting force capacity of the slip spring (Q_s) is 1.5 times as large as the resisting force capacity of the quadrilinear spring (Q_p) at γ equal to 1/120rad. The skeleton of each spring is shown in **Figure 1**. **Figure 2** shows the skeleton of each spring together with the combined one obtained for different structure models having different secant periods $T_{1/120}$. In the nonlinear dynamic response analyses, the structures are modeled as a SDOF system with 5% damping ratio. **Figure 3** shows the relationship between the resisting force and rotational angle obtained from the JR Takatori record of the 1995 Kobe earthquake for a structure with a secant natural period $T_{1/120}$ of 0.3s.

Damage model

For the wooden structure models, the damage due to a given input motion is quantified in terms of the maximum story deformation angle γ_{max} in radian, which is defined as

$$\gamma_{max} = \frac{d_{max}}{H} \tag{4}$$

where d_{max} is the maximum displacement obtained from a time history analysis, H is the story height taken as 275cm. **Figure 4** shows the distribution of γ_{max} for the 900 records with respect to different ground motion indices obtained for a structure with a secant natural period $T_{1/120}$ of 0.3s. After obtaining the γ_{max}, it is then calibrated for different damage thresholds that ranges from slight to extensive, which in terms of γ_{max} are defined as (Fire and Marine Insurance Rating Association of Japan, 1988)

$$\begin{aligned} 1/60 \le \gamma_{max} < 1/30 &: \text{ Slight,} \\ 1/30 \le \gamma_{max} < 1/15 &: \text{ Moderate,} \\ 1/15 \le \gamma_{max} &: \text{ Extensive} \end{aligned} \qquad \text{(5a, b, c)}$$

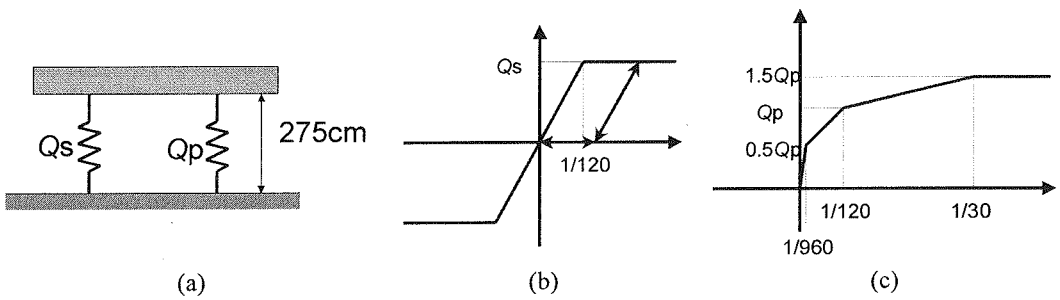

Figure 1. (a) Physical model of a wooden structure and skeleton curves for the both (b) slip spring and (c) quadrilinear spring used in the wooden structure model

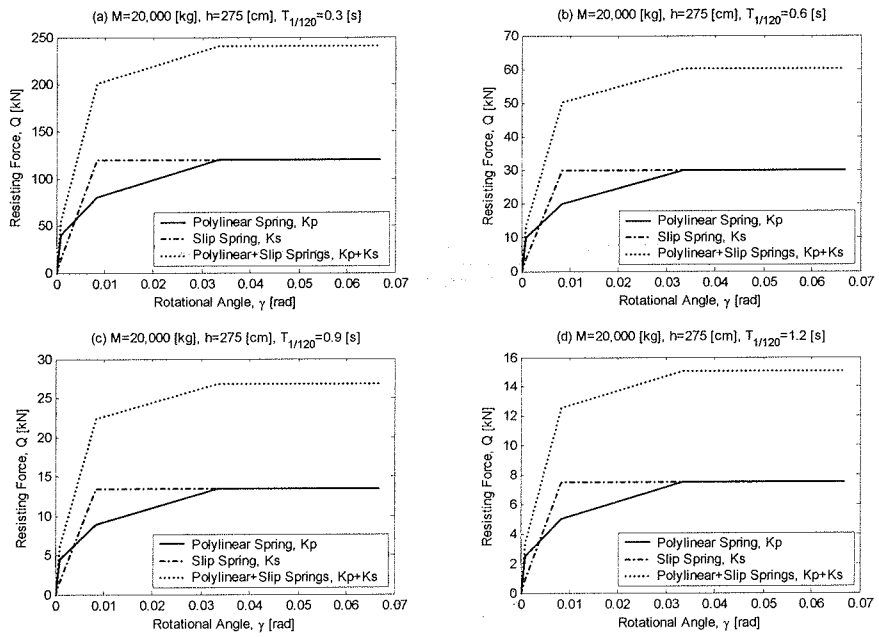

Figure 2. Skeleton curves for the wooden structure models having different periods $T_{1/120}$

It should be noted that the structure and damage models employed in this study are rather simple. However, the main purpose of this paper is to demonstrate the characteristics of the physical parameters of the earthquake ground motion in terms of the damage of the wooden structures, and more sophisticated models can be introduced in a future study.

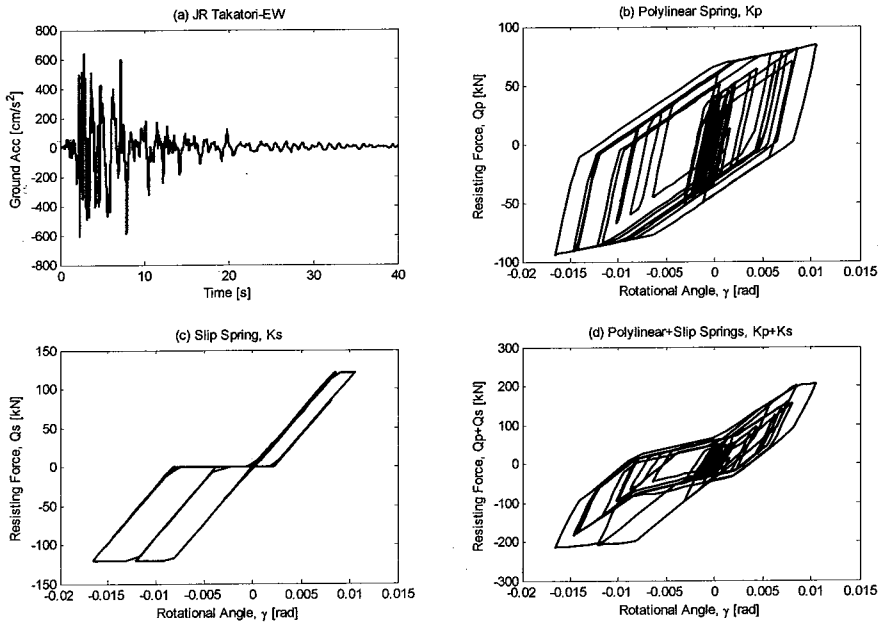

Figure 3. Resisting force vs. rotational angle relationship for a wooden structure with a natural period $T_{1/120}$ equal to 0.3s obtained from the JR Takatori-EW record of the 1995 Kobe earthquake

ACCURACY INDICATOR OF GROUND MOTION INDICES TO DISTINGUISH DAMAGE

A damage state, whether the maximum story displacement angle exceeds a damage threshold, can be considered as a binary dependent variable, which is the response function of a ground motion index. In order to identify quantitatively the input parameters that have a greater influence on the structure damage, a logit model is employed in this study, which is given as (Neter *et al.*, 1989)

$$P_d(X) = \frac{e^{aX+b}}{1+e^{aX+b}} \tag{6}$$

where $P_d(X)$ is the probability of exceeding a damage threshold, X is the ground motion index, and a and b are the regression coefficients. **Figures 5(a)-(e)** show the regression logistic curves for a damage threshold $\gamma_{\max}$ equal to 1/30rad obtained with respect to different ground motion parameters for a structure with a natural period $T_{1/120}$ of 0.4s. Since several ground motion indices with different units are considered, it is not realistic to compare the logistic curves obtained from regression analyses. To address this problem, the logistic curves obtained with respect to different ground motion parameters are normalized by

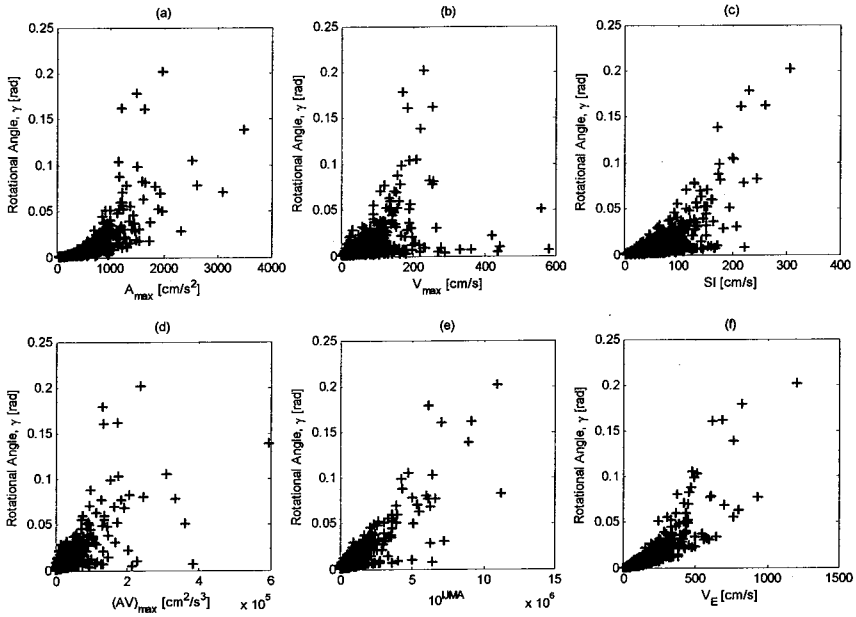

Figure 4. Distribution of story displacement angle with respect to different ground motion parameters obtained from 900 records for a structure with a secant natural period $T_{1/120}$ equal to 0.3s

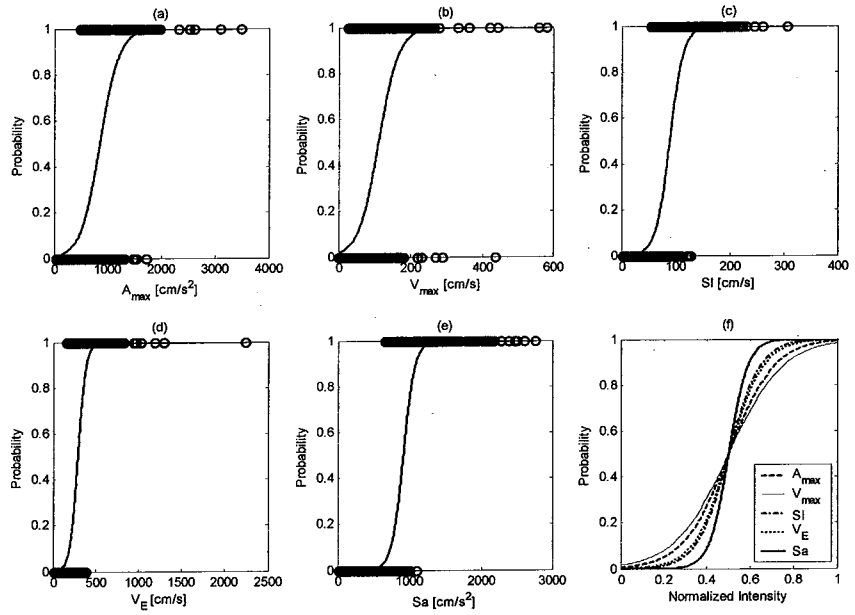

Figure 5. Logistic curves for a damage threshold γ equal to 1/30rad with respect to different ground motion indices obtained for a structure with a secant natural period $T_{1/120}$ equal to 0.4s

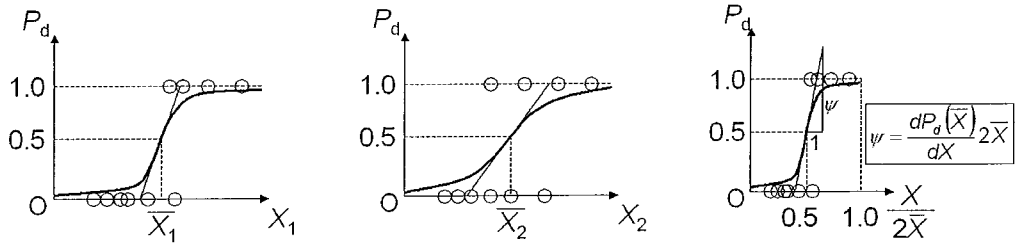

(a) (b) (c)

Figure 6. Slopes at 50% probability point of the regression logistic curves for different ground motion parameters (a) and (b), and (c) the normalized slope ψ by $X/(2\overline{X})$ at 50% probability point of the logistic curve for a given ground motion parameter X. The mathematical definition of ψ is also shown in the graph.

$$Y = \frac{X}{2\overline{X}} \tag{7}$$

so that they can be compared since all the indices are now converted to dimensionless unit. Note that the $\overline{X}$ refers the value of any ground motion index corresponding to 50% probability of the logistic curve. **Figure 5(f)** shows the logistic curves obtained for a damage threshold γ_{max} equal to 1/30rad with respect to the normalized indices of different ground motion indices for a structure with a secant natural period $T_{1/120}$ of 0.4s. Note that S_a in **Figures 5(e)** and **(f)** is calculated for a spectral period of 0.6s with 20% damping ratio.

The slope at the 50% probability point of the regression logistic curve indicates the distinction ability of the damage state, i.e., exceeding the damage threshold or not. Comparing **Figures 6(a)** and **(b)**, the large slope means that the damage states change clearly at $\overline{X}$ according to the size of X. On the other hand, the small slope suggests that the damage states are mixed around $\overline{X}$. Hence, a higher slope of the logistic curve obtained for a given ground motion index implies that it has a higher correlation with the structure damage. It can be seen (**Figure 5(f)**) that the logistic curve obtained with respect to S_a shows a higher slope at the 50% probability point than any of other indices, and it indicates that S_a has the highest correlation with the structure damage among them, and *SI* follows it. Note that the logistic curve is almost linear in the 20%-80% probability range (Neter *et al.*, 1989). The slope at the 50% probability point of the regression logistic curve with respect to the normalized index is referred as the normalized slope ψ, and a graphical representation regarding how to obtain the ψ is shown in **Figure 6(c)**. In this objective, first, the slope of the logistic curve of **Equation (6)** is obtained as

$$\frac{d}{dX} P_d(X) = \frac{ae^{aX+b}}{\left(1+e^{aX+b}\right)^2} \tag{8}$$

Equation (6) can also be transformed into a linear form by taking the logarithm at the both sides, which is derived as

$$\log_e \frac{P_d(X)}{1-P_d(X)} = aX + b \tag{9}$$

The $\overline{X}$ is obtained by using **Equation (9)** as

$$\overline{X} = \frac{1}{a}\left(\log_e \frac{0.5}{1-0.5} - b\right) = -\frac{b}{a} \tag{10}$$

The slope corresponding to $\overline{X}$ is then obtained by using **Equations (8)** and **(10)** as

$$\frac{d}{dX} P_d\left(\overline{X}\right) = \frac{d}{dX} P_d\left(-\frac{b}{a}\right) = \frac{a e^{a(-b/a)+b}}{\left(1+e^{a(-b/a)+b}\right)^2} = \frac{a}{4} \tag{11}$$

Finally, using **Equations (10)** and **(11)**, the ψ is obtained as

$$\psi = \frac{dP_d\left(\overline{X}\right)}{dX} 2\overline{X} = \frac{a}{4} \cdot 2\left(-\frac{b}{a}\right) = -\frac{b}{2} \tag{12}$$

Note that ψ is proportional to the reciprocal of the standard deviation with respect to the density function of the normalized $P_d(X)$.

COMPARISON OF GROUND MOTION INDICES

Normalized slope ψ spectra

It has already been mentioned that the regression logistic curve gives the idea that a higher slope at the 50% probability point indicates a better correlation of the structure damage with respect to a given ground motion index. The same concept holds true in case of the normalized slope ψ, which implies that a higher ψ means a higher correlation of the structure damage with respect to a given ground motion index. Since twenty-five wooden structures with natural periods $T_{1/120}$ ranging from 0.1s to 2.5s are considered in this study, it is possible to plot the ψ with respect to natural period $T_{1/120}$, which is defined as ψ spectra. Considering the diversity of the natural periods of existing wooden structures, it is necessary to see how the ψ differs for different structures having different natural periods. Note that due to the convergence problem, the ψ for structures having $T_{1/120}$ equal to 0.1s and 0.2s, respectively, are excluded from the data set because these stiff structures did not yield large displacements.

Figure 7 shows the ψ spectra obtained with respect to different ground motion indices for different damage thresholds γ. It can be seen (**Figure 7(c)**) that *SI* shows a higher level of ψ compared to other indices for the secant natural periods $T_{1/120}$ around 0.5s, and the peaks of ψ for three different damage thresholds γ= 1/60, 1/30, and 1/15rad with respect to *SI* appear at 0.7, 0.6, and 0.5s, respectively. The next higher level of ψ can be seen (**Figure 7(f)**) with respect to V_E. **Figure 8** shows the ψ spectra for a damage threshold γ equal to 1/60rad with respect to S_a, S_v, and S_d for different spectral period $T_{spectra}$ with 20% damping ratio. It can be seen (**Figure 8**) that the ψ is higher with respect to both S_a and S_d than S_v, and ψ spectra obtained with respect to both S_a and S_d seem to be very similar. Similar trend is also found with respect to other damage thresholds γ and as well as with 5% and 10% damping ratio. From this observation, it can be said that S_a and S_d have a better correlation with the structure damage than S_v. Although both S_a and S_d have a better correlation with the structure damage, S_a is chosen for simplicity rather than S_d in this study.

Since damping ratio plays an import role with the amplitude of S_a, S_v, and S_d, it is also necessary to see which damping ratio provides S_a, S_v, and S_d to have a higher correlation with the structure damage. In this objective, the ψ spectra is also obtained for the three different damage thresholds with respect to S_a, S_v, and S_d of three different damping ratios, 5%, 10% and 20%. **Figure 9** shows the ψ spectra with respect to S_a for a damage threshold γ equal to 1/30rad with the three different damping ratios for four different spectral periods $T_{spectra}$ = 0.3, 0.6, 0.9, and 1.2s. It can be seen that ψ obtained with respect to

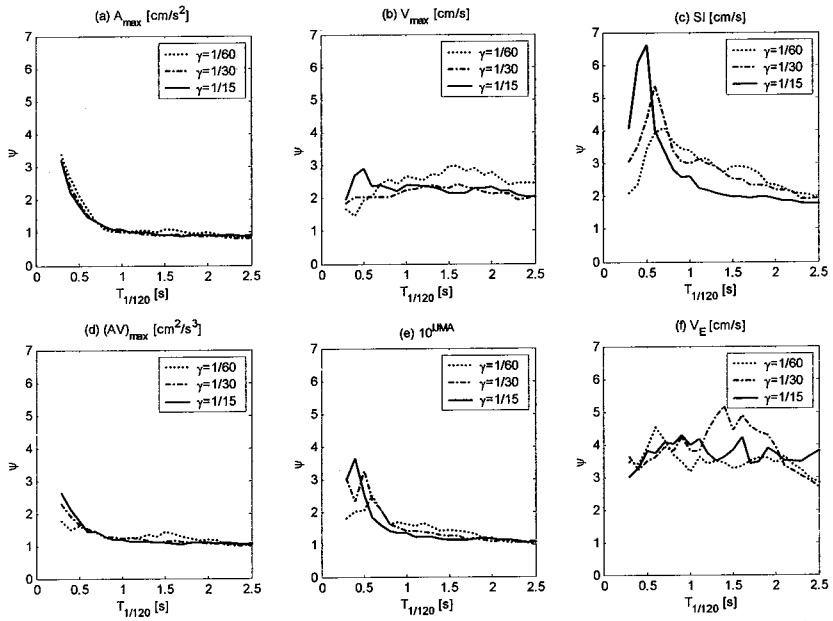

Figure 7. Normalized slope ψ spectra for different damage thresholds γ with respect to different ground motion indices

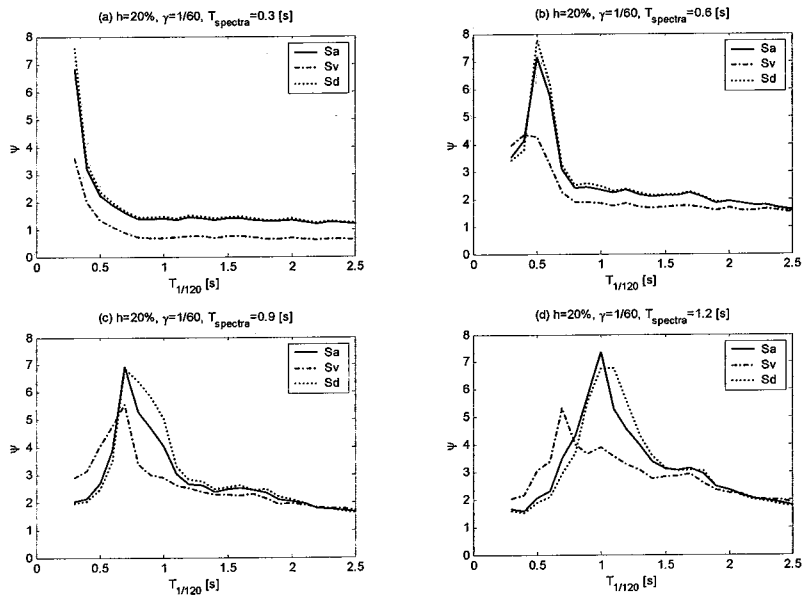

Figure 8. Normalized slope ψ spectra for a damage threshold γ equal to 1/60rad with respect to acceleration, velocity, and displacement response spectra for different spectral period with 20% damping ratio

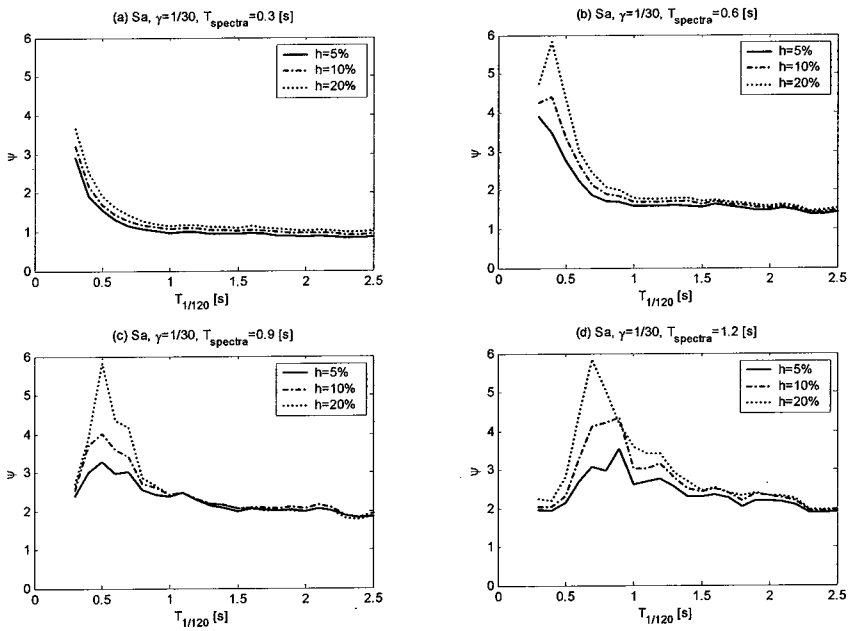

Figure 9. Normalized slope ψ spectra for a damage threshold γ equal to 1/30rad with respect to acceleration response spectra for different spectral period with different damping ratio

S_a with 20% damping ratio is mostly higher than the one obtained with 5% and 10% damping ratio. Similar trend is also observed for other damage thresholds and as well as with respect to both S_v and S_d. It means that 20% damping ratio provides S_a, S_v, and S_d to have a higher correlation with the structure damage. Based on the above two observations, S_a and S_d can be considered as better indices than S_v to correlate with the structure damage, and that it should be calculated with 20% damping ratio. Note that there are two kinds of period: one is the spectral period $T_{spectra}$, and the other one is the structural period $T_{1/120}$, which is the secant natural period of a nonlinear model for a wooden structure.

Acceleration response spectrum S_a considering period elongation

From **Figures 7**, **8** and **9**, it can be also noticed that each ψ spectra curve shows a peak or the largest value with respect to any given ground motion index. If $T_{spectra}$ is carefully selected to have these peaks, it is expected that S_a of this $T_{spectra}$, should have very large ψ. In this objective, ψ is obtained with respect to S_a for different combinations of $T_{spectra}$ and $T_{1/120}$. **Figure 10** shows the ψ spectra for different damage thresholds with respect to S_a with 20% damping for different combination of $T_{spectra}$ and $T_{1/120}$. **Figures 10(a), (b),** and **(c)** use $T_{spectra}$ in the horizontal axis, while **Figures 10(d), (e),** and **(f)** use $T_{1/120}$.

In **Figure 10(a)**, it can be seen that for a damage threshold γ equal to 1/60rad, the peak of ψ for a structure period $T_{1/120}$ of 0.3s can be seen at $T_{spectra}$ equal to 0.4s. It implies that the peak of ψ for a structure period $T_{1/120}$ equal to 0.3s is found at an elongated $T_{spectra}$ equal to 0.4s. Similar trend is also observed for other structural periods $T_{1/120}$ and as well as for other damage thresholds. Now, if one looks at **Figure 10(d)**, then it can be seen that for a damage threshold γ equal to 1/60rad, the peak of ψ for a spectral period $T_{spectra}$ of 0.3s can be seen at $T_{1/120}$ equal to 0.2s. It implies that the peak of ψ for a spectral period $T_{spectra}$ of 0.3s is found at a shortened $T_{1/120}$ equal to 0.2s. Similar trend is also observed for other spectral periods $T_{spectra}$ and as well as for other damage thresholds. These observations give the idea that when a particular structural period is considered then S_a should be calculated at an elongated spectral period and vice versa. Therefore, it necessitates to knowing the relationship

between the structural period $T_{1/120}$ and the spectral period $T_{spectra}$, which is obtained with respect to the peak of ψ for different combinations of ψ spectra.

Figures 11(a), (b) and **(c)** shows the relationship between $T_{1/120}$ and $T_{spectra}$ for a damage threshold γ equal to 1/60, 1/30, and 1/15rad, respectively. Since these scatter plots are based on the peaks of ψ spectra derived from combinations of discrete $T_{spectra}$ and $T_{1/120}$, the scatter points distribute on the lattice of 0.1s intervals. In **Figure 11(a)**, it can be seen that $T_{spectra}$ can be obtained from $T_{1/120}$ by using a scale factor or period elongation coefficient α equal to 1.26. Similarly, α for the other damage thresholds γ equal to 1/30 and 1/15rad are obtained as 1.66 and 2.29, respectively. **Figure 11(d)** shows the comparison of the regression lines for the three different damage thresholds. It can be seen that the higher the damage level, the higher the elongation of $T_{spectra}$. When the periods ratio between the secant natural period at a damage threshold and the secant natural period at story displacement 1/120 is considered, similar trend can be observed to the elongation coefficient α; the derived ratio is referred as the theoretic elongation coefficient.

Figure 12 shows the relationship between the period elongation coefficient α with respect to different damage thresholds obtained from the both regression analysis and theoretic formula. It can be seen that α obtained from the both analysis and theory with respect to different damage thresholds are very similar. Hereafter, α obtained from the numerical analysis is referred as the period elongation factor; α depends on the considered damage threshold. Based on this observation, the ψ for different damage thresholds with respect to S_a is calculated by linear interpolation using the elongated spectral period $T_{spectra}$, which is given as

$$T_{spectra} = \alpha T_{1/120} \tag{13}$$

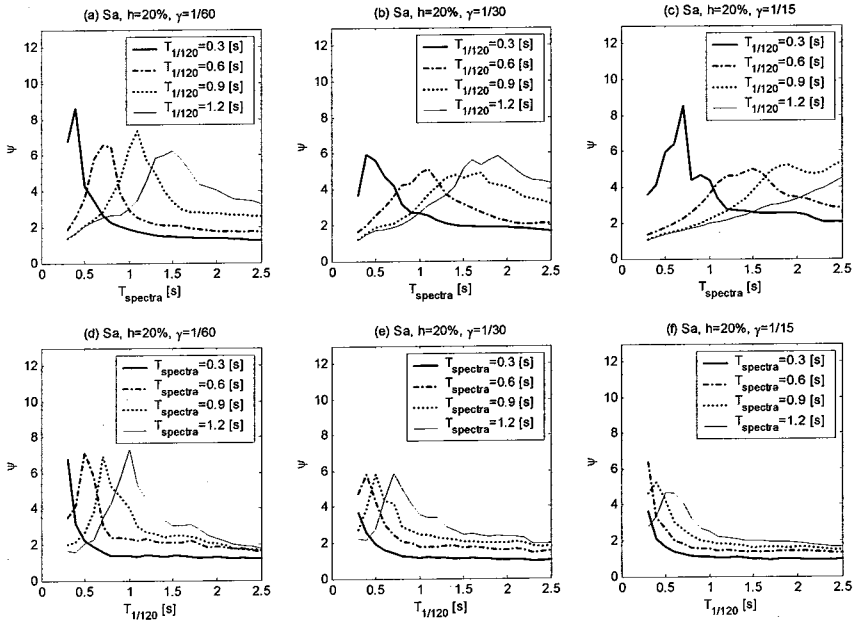

Figure 10. Normalized slope ψ spectra for different damage thresholds γ with respect to acceleration response spectra for different combinations of spectral and structural period with 20% damping ratio

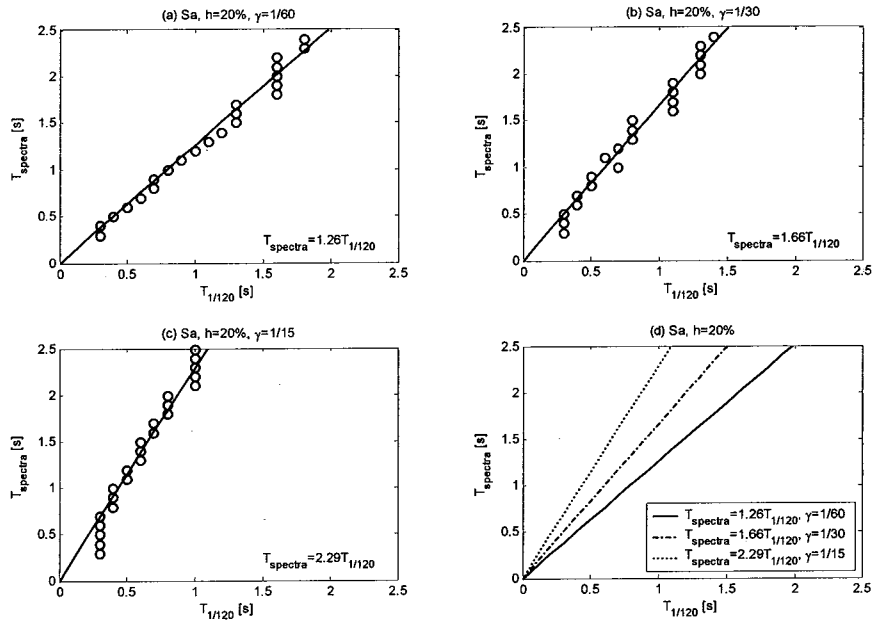

Figure 11. Relationship between spectral period and structural period for different damage thresholds γ with respect to acceleration response spectra with a 20% damping ratio

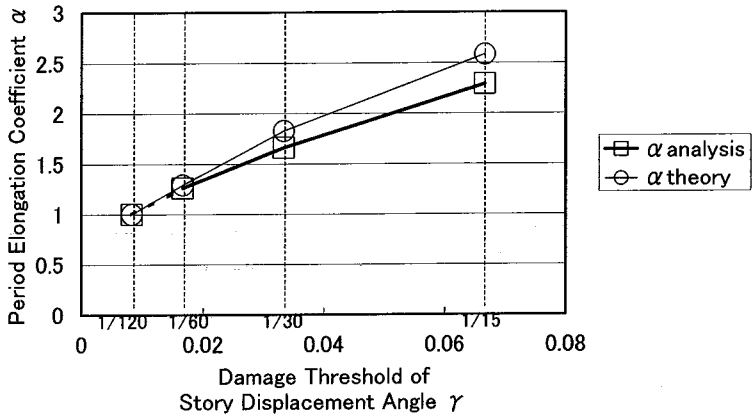

Figure 12. Relationship between period elongation coefficient α and damage threshold of story displacement angle γ obtained with respect to the both numerical analysis and theoretical formula

where α equal to 1.26, 1.66, and 2.29 for the damage thresholds γ equal to 1/60, 1/30, and 1/15rad, respectively. After obtaining the ψ with respect to S_a for the elongated spectral period $T_{spectra}$, it is then compared with the ones obtained with respect to other ground motion indices.

Comparison of ψ for different ground motion indices

In the previous section, S_a of the elongated period with 20% damping ratio became a promising candidate of ground motion indices highly correlated with the wooden structures damage. It has been observed that *SI* shows a higher correlation with the structure damage than other parameters for the period around 0.5s, and the next higher correlation is seen with respect to V_E in **Figure 7**. In order to examine whether the S_a of the elongated period shows higher correlation than them, the ψ spectra are compared. **Figure 13** shows the comparison of ψ obtained for the three different damage thresholds with respect to all the parameters considered in this study.

It should be noted that the ψ for different damage thresholds with respect to S_a is obtained by linear interpolation using the elongated spectral period $T_{spectra}$ of **Equation (13)**. It should also be noted that the structural period $T_{1/120}$ for different damage thresholds is limited up to the level that gives the elongated period $T_{spectra}$ less than or equal to 2.5s since the range of structural period for analysis is limited to 2.5s, and the maximum limit of $T_{1/120}$ of **Equation (13)** is found around 1.0s for the damage threshold γ equal to 1/15rad (**Figure 11(c)**). It can be seen (**Figure 13**) that ψ obtained with respect to S_a mostly shows higher amplitudes for the all damage thresholds compared to the ones obtained with respect to other indices.

WEIGHTED SPECTRUM INTENSITY

The preceding sections give an overall idea regarding which ground motion parameter has a higher correlation with the structure damage and in which condition. Among all the parameters, S_a (h = 20%) mostly shows the better performance for the all damage thresholds Based on this observation, Weighted Spectrum Intensity (*WSI*) is proposed as the ground motion index that might give better performance with respect to the distinction of the wooden structures damage, and it is defined as

$$WSI = \int_{0.3}^{1.0} \frac{w(T_{1/120})S_a(h=20\%, T=\alpha T_{1/120})}{2\overline{S_a}(h=20\%, T=\alpha T_{1/120})} dT_{1/120} \tag{14}$$

where $\overline{S_a}$ is the normalization coefficients of acceleration response spectra (see **Equation (7)**) as is shown in **Figure 14**, and α is the period elongation factor, which is dependent on the damage threshold. $w(T_{1/120})$ is the probability density function of the wooden structures with respect to the secant natural period at story displacement angle γ equal to 1/120rad. The function $w(T_{1/120})$ is used in order to take a weighted average between the period range from 0.3s to 1.0s, in which most of wooden structures exists. The steps for calculating the *WSI* of **Equation (14)** is given as:

1. Get the acceleration time history of an earthquake record and calculate the response spectrum $S_a(h=0.2, T)$ for T = 0.3, 0.4, ..., 2.5s.
2. Interpolate S_a of **Step (1)** for $T = \alpha T_{1/120}$ ($T_{1/120}$ = 0.3, 0.4, ..., 1.0s), in which the period elongation factor α =1.26, 1.66, and 2.29 for the damage thresholds γ = 1/60, 1/30, and 1/15, respectively.
3. Derive and interpolate the normalization coefficients of the acceleration response spectrum $\overline{S_a}(h=0.2, T=\alpha T_{1/120})$ ($T_{1/120}$ = 0.3, 0.4, ..., 1.0s) from **Figure 14**.
4. Assume the weight function $w(T_{1/120})$ ($T_{1/120}$ = 0.3, 0.4, ..., 1.0s), or elicit $w(T_{1/120})$ statistically depending on the wooden structures in a target area.
5. Finally, obtain the *WSI* using **Equation (14)** by numerical integration between the periods $T_{1/120}$ equal to 0.3s to 1.0s.

The schematic diagram for the calculation of the *WSI* is also shown in **Figure 15**. The *WSI* may be a very useful tool and conveniently be used in damage estimation of wooden structures due to an earthquake.

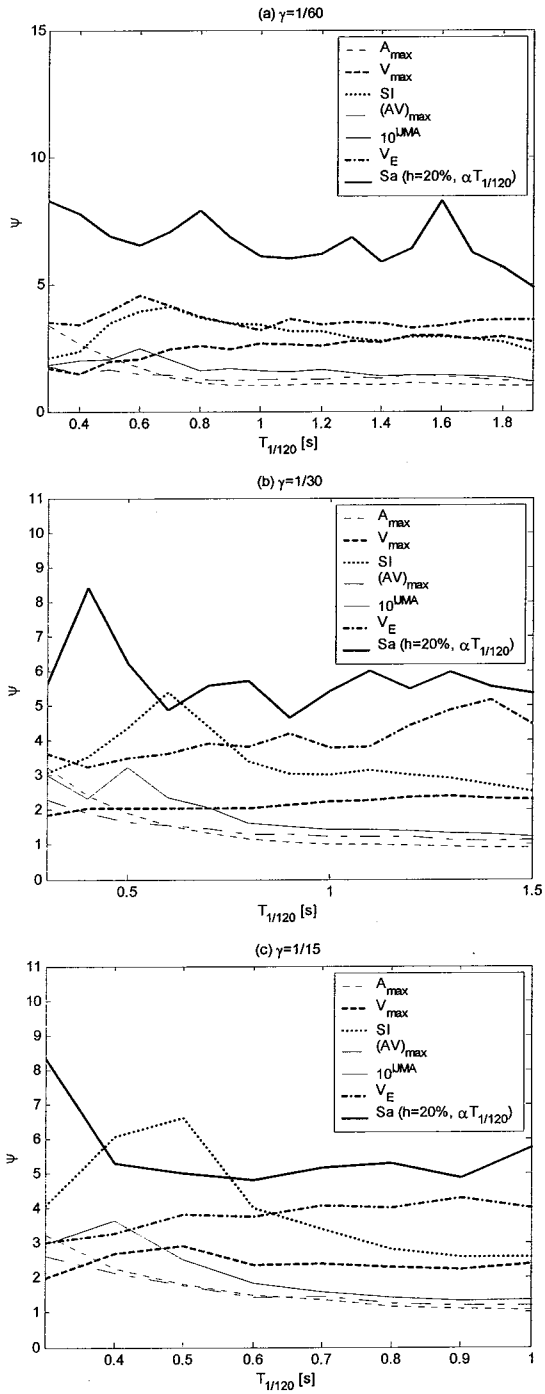

Figure 13. Comparison of the normalized slope ψ spectra obtained for different damage thresholds γ with respect to different ground motion indices

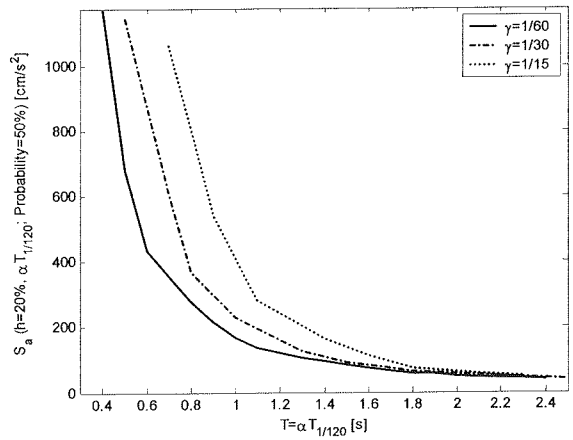

Figure 14. Distribution of the normalization coefficients of acceleration response spectra $\overline{S}_a(h=20\%, T=\alpha T_{1/120})$ for different damage thresholds γ where the elongated period $T=\alpha T_{1/120}$ and α= 1.26, 1.66, and 2.29.

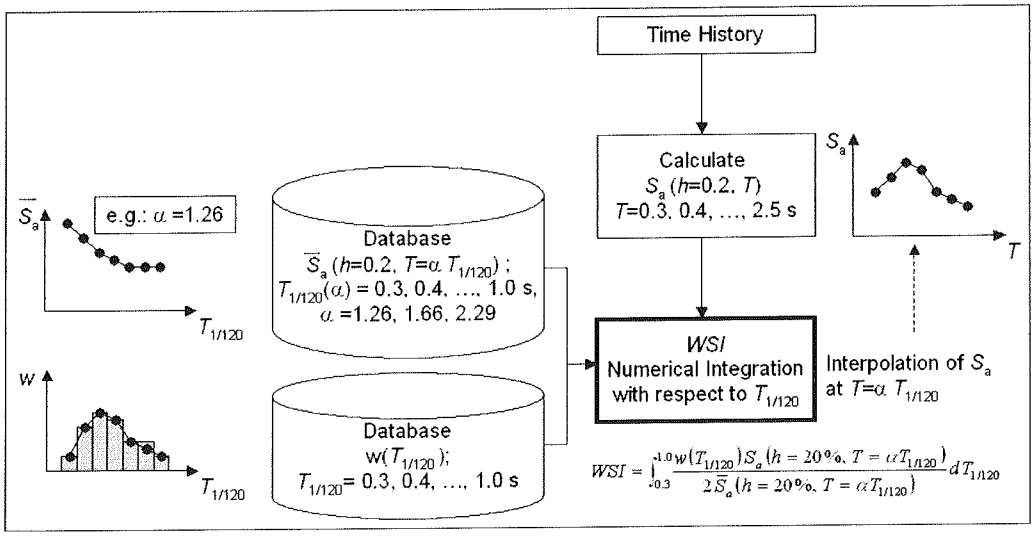

Figure 15. Schematic diagram to obtain the new seismic damage parameter Weighted Spectrum Intensity *WSI*. The mathematical definition of *WSI* is also shown in the diagram.

CONCLUSIONS

To study the relationship between ground motion indices and wooden structures damage, numerical analyses are conducted. The wooden structure models having secant natural periods at the story displacement angle equal to 1/120rad within the range of 0.1s to 2.5s were considered, and the maximum story displacement angles for the selected structures were obtained by performing a nonlinear time history analysis considering nine hundred records as the input motion. A logistic

regression analysis was performed to obtain the correlation between the structure damage and ground motion parameters for different damage thresholds. The slope at 50% probability of the regression logistic curve for a normalized ground motion index, ψ, was introduced as an indicator for better correlation of the structure damage. It was observed that acceleration response spectra with 20% damping ratio and with an elongated spectral period along with the damage threshold shows the better performance correlated with the structure damage. A new ground motion index, i.e., the weighted spectrum intensity *WSI* was also developed, which considers the natural period distribution of wooden structures and period elongation effect due to nonlinear behaviors. *WSI* may be a very useful parameter and conveniently be used for earthquake damage estimation of wooden structures. However, a validity study is required to show the accuracy of damage estimation and practical usefulness of *WSI*. In addition, since only single-storied wooden structures were considered in this study, hence, to draw a solid conclusion, it is necessary to consider multi-storied wooden structures, and a further study is recommended in this regard.

REFERENCES

Fire and Marine Insurance Rating Association of Japan (1988). "Study on the damage ratio of wooden houses, part-2." *Research Report for Earthquake Insurance*, Vol. 22, 61-104 (in Japanese).

Housner, G. W. (1959). "Behavior of structures during earthquakes." *Journal of the Engineering Mechanics*, ASCE, Vol. EM4, 109-129.

Japan Meteorological Agency (JMA, 1996). *Shindo wo Shiru* (Note on the JMA seismic intensity). *Gyosei*, 46-224 (in Japanese).

Kamiyama, M. (1996): "Spectral characteristics of strong ground motions in terms of peak values." *Journal Structural Mechanics and Earthquake Engineering*, JSCE, No. 531/I-34, 35-49.

Katayama, T., Sato, N. and Saito, K. (1988). "SI-sensor for the identification of destructive earthquake ground motion." *Proc. of the 9th World Con. Earthquake Engineering*, Vol. 7, 667-672.

Loh, C-H., Lee, Z-K., Wu, T-C. and Peng, S-Y. (2000). "Ground motion characteristics of the Chi-Chi earthquake of 21 September 1999." *Earthquake Engineering and Structural Dynamics*, Vol. 29, 867-897.

Molas, G. L. and Yamazaki, F. (1995). "Neural networks for quick earthquake damage estimation." *Earthquake Engineering and Structural Dynamics*, Vol. 24, No. 4, 505-516.

Nakamura, S., Murono, Y., and Ashiya, K. (2002). "Basic study for estimating nonlinear response of structure based on energy index of earthquake ground motion." *Journal of Structural Mechanics and Earthquake Engineering*, JSCE, No. 710/I-60, 399-411

Neter, J., Wasserman, W. and Kutner, M. H. (1989). *Applied linear regression models*, IRWIN, Boston, USA.

Suzuki, Y. and Nakaji, H. (1997). "Seismic response and resistance of wooden structures under strong earthquakes." *Proc. of the 2nd Comprehensive Symposium on Urban Disasters Caused by Near-Field Earthquakes*, Tokyo, Japan, 211-214 (in Japanese).

Tong, H. and Yamazaki, F. (1995). "A relationship between seismic ground motion severity and house damage ratio." *Proc. of the 4th US Conference on Lifeline Earthquake Engineering*, ASCE, 33-40.

Trifunac, M. D. and Brady, A. G. (1975). "A study of the duration of strong earthquake ground motion." *Bulletin of the Seismological Society of America*, vol.65, 581-626.

Uang, C-M. and Bertero, V. V. (1990). "Evaluation of seismic energy in structures." *Earthquake Engineering and Structural Dynamics*, Vol. 19, 77-90.

Yamazaki, F., Motomura, H. and Hamada, T. (2000). "Damage assessment of expressway networks in Japan based on seismic monitoring." *12th World Conference on Earthquake Engineering*, CD-ROM, Paper No. 0551.